Original Research

Real-Time Flow MRI of the Aorta at a Resolution of 40 msec

Arun Joseph, MSc,[1]* Johannes T. Kowallick,[2] Klaus-Dietmar Merboldt, PhD,[1] Dirk Voit, PhD,[1] Sebastian Schaetz, Dipl. Inf,[1] Shuo Zhang, PhD,[1] Jan M. Sohns, MD,[2] Joachim Lotz, MD,[2] and Jens Frahm, PhD[1]

Purpose: To evaluate a novel real-time phase-contrast magnetic resonance imaging (MRI) technique for the assessment of through-plane flow in the ascending aorta.

Materials and Methods: Real-time MRI was based on a radial fast low-angle shot (FLASH) sequence with about 30-fold undersampling and image reconstruction by regularized nonlinear inversion. Phase-contrast maps were obtained from two (interleaved or sequential) acquisitions with and without a bipolar velocity-encoding gradient. Blood flow in the ascending aorta was studied in 10 healthy volunteers at 3 T by both real-time MRI (15 sec during free breathing) and electrocardiogram (ECG)-synchronized cine MRI (with and without breath holding). Flow velocities and stroke volumes were evaluated using standard postprocessing software.

Results: The total acquisition time for a pair of phase-contrast images was 40.0 msec (TR/TE = 2.86/1.93 msec, 10° flip angle, 7 spokes per image) for a nominal in-plane resolution of 1.3 mm and a section thickness of 6 mm. Quantitative evaluations of spatially averaged flow velocities and stroke volumes were comparable for real-time and cine methods when real-time MRI data were averaged across heartbeats. For individual heartbeats real-time phase-contrast MRI resulted in higher peak velocities for values above 120 cm s^{-1}.

Conclusion: Real-time phase-contrast MRI of blood flow in the human aorta yields functional parameters for individual heartbeats. When averaged across heartbeats real-time flow velocities and stroke volumes are comparable to values obtained by conventional cine MRI.

PHASE-CONTRAST MAGNETIC RESONANCE IMAGING (MRI) of cardiovascular blood flow is an established tool of clinical utility in the assessment of cardiac function which is performed using electrocardiogram (ECG)-synchronized cine acquisitions with or without breath holding (1–5). On the other hand, real-time MRI studies of blood flow show some promise in the ability to overcome problems due to irregular heartbeats or poor respiratory control, improve patient compliance, and provide new opportunities for monitoring physiologic responses to stress and exercise (for an early example, see (6)). However, although real-time techniques have become a research focus for both cardiovascular MRI (7–12) and phase-contrast flow MRI (13–18), many proposals offer only limited spatiotemporal resolution and/or low image quality that hampers clinical acceptance. Most recently, we presented a new principle for phase-contrast flow MRI in real time which relies on highly undersampled radial fast low-angle shot (FLASH) acquisitions in conjunction with image reconstruction by regularized nonlinear inversion (19). The aim of this study was to further develop this idea toward a quantitatively reliable through-plane flow MRI method and to demonstrate its feasibility by measuring blood flow in the human aorta in direct comparison to established cine recordings.

MATERIALS AND METHODS

This study was approved by the Institutional Review Board and all participants gave written informed consent before each examination. Ten male volunteers (25.2 ± 2.0 years [mean ± standard deviation]; range 20–30 years) with no known illness were recruited from the local university. MRI studies were conducted at 3 T with the use of a commercial MRI system (Tim Trio, Siemens Healthcare) and a standard 32-channel

Figure 1. Schematic sequence diagram for real-time phase-contrast MRI of through-plane flow using radial FLASH (G_{read1}, G_{read2}) without and with a bipolar velocity-encoding gradient (G_{venc}, interleaved version). In practice, the flow-encoding gradient is combined with overlapping parts of the slice-selection gradient (G_{slice}). RF = radiofrequency pulse, TE = echo time, TR = repetition time, n = number of radial spokes.

cardiac coil (anterior and posterior parts with 16 array elements each). Conventional MRI-compatible ECG recordings served for retrospective triggering of cine studies and provided ECG time stamps for real-time images to facilitate the evaluation of functional parameters.

Real-Time Phase-Contrast MRI

Real-time MRI based on highly undersampled gradient-echo acquisitions with regularized nonlinear inverse reconstruction (10–12) was recently extended to phase-contrast flow MRI (19). As demonstrated in Fig. 1, the further modified technique proposed here consists of a radial FLASH sequence with a motion-compensated slice-selective gradient and a bipolar flow-encoding gradient (zero-maximum version) which may be applied in an interleaved (every other repetition interval) or sequential fashion (every other image acquisition). In order to shorten the gradient-echo time as much as possible the implementation was restricted to through-plane flow with flow-encoding gradients that overlap with slice and read gradients. These developments resulted in an acquisition time of only 40 msec (ie, for both the magnitude image and phase-contrast map) and a nominal in-plane resolution to 1.3 mm.

The slew rates of the magnetic field gradients were set to lower than maximal values in order to avoid peripheral nerve stimulation in line with vender calculations. In order to achieve T1 contrast the radial FLASH sequence used radiofrequency (RF) spoiling and in addition exploited the inherent gradient spoiling of a radial MRI sequence. In contrast to Cartesian sampling, this powerful spoiling capacity emerges from the change of the frequency-encoding gradients in every repetition interval.

T1-weighted RF-spoiled images were continuously acquired with the following parameters: repetition time TR = 2.86 msec, echo time TE = 1.93 msec, flip angle 10°, field of view (FOV) 192×192 mm^2, in-plane resolution 1.3×1.3 mm^2, slice thickness 6 mm, VENC = 200 cm s^{-1}. Individual images were obtained from seven radial spokes (144 data samples) equally distributed to homogeneously sample k-space, while five consecutive acquisitions used complementary sets of radial spokes. Relative to the Nyquist limit of $144 \times \pi/2 = 226$, the degree of undersampling refers to a factor of 32. Two-fold frequency oversampling allowed for the use of a small FOV without artifacts. All real-time acquisitions were performed during free breathing for a period of 15 seconds corresponding to about 12 to 15 heartbeats. Corresponding datasets resulted in 375 magnitude images and phase-difference maps.

Online Image Reconstruction

The development of a "bypass" computer equipped with eight graphical processing units (GPUs, GeForce GTX 580, Nvidia, Santa Clara, CA) allowed for online reconstruction and display of both magnitude images and phase-contrast maps with a slight but acceptable delay. The server was fully integrated into the commercial MRI system and invisible to the user. To achieve such image reconstructions without user interference, the measured k-space data were diverted from the vendor-supplied image calculation pipeline (ICE, Siemens) and transferred to the "bypass" computer (sysGen/TYAN Octuple-GPU, 2x Intel Westmere E5620 processor, 48GB RAM, Sysgen, Bremen, Germany) via Gigabit Ethernet. Two packs of 4 GPUs simultaneously reconstruct the two streams of images (ie, with and without a flow-encoding gradient) by using a specially developed multi-GPU programming library for real-time applications (20). For the chosen experimental conditions and the current hardware, the reconstruction and display took about 60 seconds for 375 pairs of magnitude images and phase-contrast maps. The corresponding rate of about 2×6 fps enables adequate visual control of the actual measurement. The images are automatically stored in the normal databank of the MRI scanner.

As discussed in preceding work about the nonlinear inverse reconstruction method (11,21,22), the combined estimation of image and coil sensitivities employed an additional "oversampling factor" of 1.5 on top of the 2-fold frequency oversampling during data acquisition, so that the actual reconstructions are accomplished on 3-fold the nominal FOV. Finally, while magnitude images were subjected to a temporal median filter to alleviate residual streakings, the phase images used for phase-contrast flow velocity maps were obtained without any temporal filter to achieve optimum temporal fidelity.

Cine Phase-Contrast MRI

Standard ECG-gated cine phase-contrast MRI was performed during free breathing as well as with

breath holding without navigator. The basic scan parameters for both conditions were similar: slice thickness 6 mm, flip angle $25°$, phase resolution 100%, VENC = 200 cm s^{-1}. Other parameters for cine MRI with free breathing were: TR = 20.05 msec (two acquisitions with different flow encodings, two segments), TE = 2.18 msec, 3 averages, 30 phases, FOV = 320 mm, base resolution 256, rectangular FOV phase 75%, phase oversampling 30%, in-plane resolution 1.3 mm. The parameters for cine MRI with breath holding were: TR = 46.90 msec (two acquisitions, five segments), TE = 1.92 msec, rectangular FOV phase 68.8%, no phase oversampling, base resolution 192, 1 average, 20 phases, in-plane resolution 1.7 mm. Reconstructions were performed with generalized autocalibrating partially parallel acquisition (GRAPPA) using a nominal acceleration factor of 2 and 24 reference lines defining the fully sampled k-space center. Typically, the measuring times for cine MRI with free breathing were 3.3 minutes, while cine MRI with breath holding took about 13 seconds.

Study Protocol

The examination protocol comprised cine MRI with and without breath holding as well as real-time MRI with interleaved and sequential flow encoding. Flow measurements were performed in a single oblique plane perpendicular to the ascending aorta at the level of the right pulmonary artery. All measurements were repeated three times in a pseudorandomized order. Total examination times were 30–40 minutes.

Additional studies of a static phantom (agarose gel) were performed to evaluate residual phase offsets by real-time and cine methods. These measurements used a simulated ECG from the MRI system and were repeated for each subject keeping the same conditions (image orientation, shim) as for flow MRI in the aorta.

Flow Evaluation

Functional parameters were derived from dynamic series of magnitude images and phase-contrast maps with the use of QFlow 5.4 prototype software (MEDIS Medical Imaging Systems, Leiden, The Netherlands). This version was specifically designed to extend the conventional analysis of a single (synthetic) cardiac cycle to real-time evaluations of multiple heartbeats. For the analysis of real-time MRI acquisitions 10 consecutive cardiac cycles were chosen in all cases. Functional evaluations included peak velocities, mean velocities spatially averaged over the aortic lumen, flow rates, stroke volumes, and cardiac output.

Both real-time and cine MRI movies were jointly evaluated by one radiologist (J.K., 2 years clinical experience) and one physicist (A.J.) to reduce interobserver deviations through consensus about the segmentation of the aorta. This approach was chosen to exclude putative influences of the available postprocessing software, which has not yet fully been optimized for real-time MRI conditions. The automatic propagation of a defined contour was visually controlled and if necessary manually corrected. The results obtained with and without manual contour correction were recorded as well as the durations needed for automated and manual corrections along with the total number of corrected images.

Mean phase offset values from phantom measurements were obtained using the in vivo contours of the aorta for all 10 subjects. Corresponding spatially averaged velocities were compared to the maximum encoding velocity (VENC). Because of the small values obtained for real-time MRI (see below), no phase offset corrections were performed.

Statistics

Flow parameters obtained for real-time MRI (10 heartbeats) were expressed as mean ± standard deviation. A comparison of flow parameters obtained by real-time and cine MRI methods was performed using a paired Student's t-test with $P < 0.05$ considered statistically significant. Results obtained for peak velocities and stroke volumes were further evaluated by linear correlations as well as Bland–Altman analysis to yield measures of agreement (23).

RESULTS

Technical Aspects

Figure 2 compares anatomic images and phase-contrast maps at peak systole and late diastole for cine MRI with free breathing and breath holding (top) and real-time MRI with interleaved and sequential application of the flow-encoding gradient (bottom). A dynamic representation of real-time images and phase-contrast maps for 10 consecutive heartbeats is shown in Supporting Movie 1.

Cine MRI methods with Cartesian phase encoding not only required a large FOV to avoid image aliasing, but also led to residual ghosting artifacts along the (vertical) phase-encoding direction due to phase errors from involuntary motions and pulsatile flow. The latter problem is not avoided by breath holding. In contrast, real-time images with radial encoding were free of such artifacts and exhibited only small residual streakings in peak systolic phase-contrast maps (Fig. 2, left part). In diastole (Fig. 2, right part) real-time image quality and definition of the aorta was visually better than in cine recordings.

In general, quantitative flow assessments using phase-contrast MRI rely on minimal phase offsets due to field inhomogeneities and eddy currents (24). In this study, the mean real-time MRI phase offset values derived from phantom measurements corresponded to 2.9 and 2.4 cm s^{-1} for interleaved and sequential flow encoding, respectively. These values were well below the recommended limit of 5% of the VENC value (25).

The percentage of images that needed manually corrected segmentations was $27.4 \pm 10.5\%$ and $25.6 \pm 9.3\%$ for real-time MRI with interleaved and sequential flow encoding, respectively. Corresponding values for cine MRI were even higher, yielding $47.3 \pm 21.1\%$ for breath holding and $38.1 \pm 14.1\%$ for
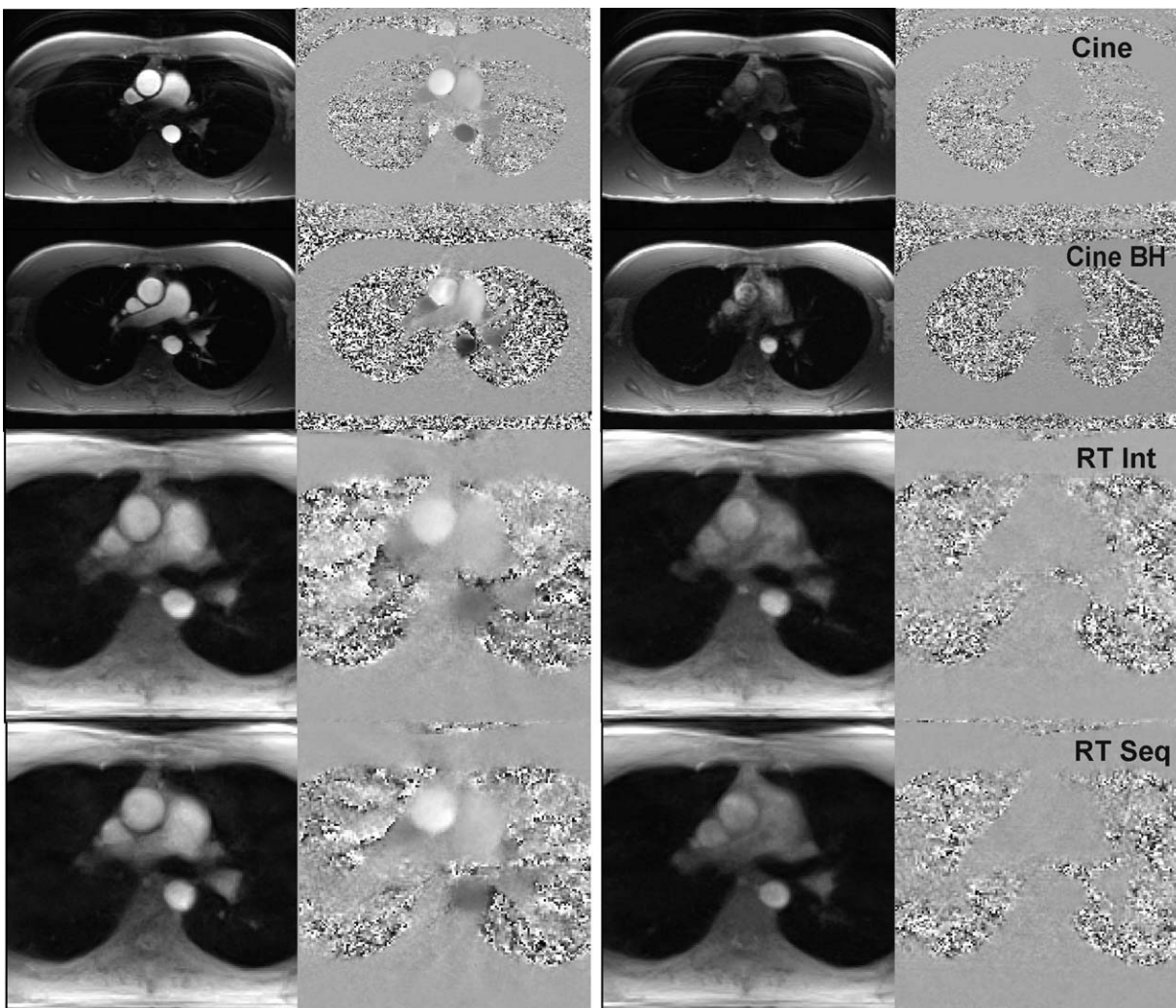
Figure 2. (Left) Peak systolic and (right) diastolic anatomic images and phase-contrast maps (single subject) as obtained by cine MRI with free breathing (Cine) and breath holding (Cine BH) as well as real-time MRI with interleaved (RT Int) and sequential (RT Seq) flow encoding.

free breathing. This is partially due to the fact that diastolic cine images present with poor contrast and therefore degrade the automated segmentation and propagation of contours. In line with these findings the durations needed for the correction of segmentation errors were 9.7 ± 4.9 minutes (interleaved) and 9.4 ± 5.1 minutes (sequential) for an average of 250 real-time images as well as 1.5 ± 0.7 minutes (free breathing) and 1.4 ± 1.3 minutes (breath holding) for an average of 30 cine images. With respect to individual heartbeats, the mean durations for both real-time MRI versions reduce to 0.9 ± 0.5 minutes, which is even faster than for cine MRI.

Table 1 summarizes the results for the maximum mean flow velocities that are spatially averaged over the lumen of the ascending aorta. No significant differences were observed for real-time vs. cine acquisitions when comparing data for 300 heartbeats (realtime MRI) and 30 synthetic cycles (cine MRI) across subjects—neither without nor with manual correction. Even after manual correction, the values for real-time MRI were almost identical to those obtained for cine

MRI with breath holding, while only minor deviations (mean bias of -2.6%) occurred for cine MRI studies with free breathing. On the other hand, when studying the influence of manually corrected segmentations, no significant differences were obtained for cine MRI, whereas both real-time MRI methods resulted in slightly but significantly higher values after correction (paired t-test, $P = 0.02$).

Aortic Blood Flow

Figure 3 shows the mean flow velocities in the ascending aorta of a single subject for 10 consecutive heartbeats using real-time MRI with interleaved flow encoding (top trace). The temporal fluctuation of the maximum velocities for successive cardiac cycles reflects differences in relation to inspiratory and expiratory phases of the breathing cycle (19), which in this example corresponds to 3 to 4 seconds or a rate of 15 to 20 min^{-1}. Although no major velocity differences were seen for interleaved and sequential flow encoding when combining data from 30 heartbeats

Table 1
Maximum Spatially Averaged Flow Velocities in the Ascending Aorta

	Fully automated analysis	After manual correction
Cine MRI[a] Free Breathing	80.4 ± 7.3	80.6 ± 7.4
Cine MRI[a] breath holding	83.0 ± 8.7	82.9 ± 8.8
Real-time MRI[b] interleaved flow encoding	80.9 ± 10.4	82.8 ± 11.2
Real-time MRI[b] sequential flow encoding	80.8 ± 10.1	82.6 ± 11.0

Values are given in cm s^{-1} (mean ± SD) and represent the maximum mean flow velocities averaged over the lumen of the aorta.
[a]10 subjects, 3 repetitions.
[b]10 subjects, 3 repetitions, 10 heartbeats.

(lower traces), the sequential scheme identifies slightly negative velocities for a brief period immediately after systole, at least for a few cardiac cycles.

Figure 4 compares the peak velocities (single voxel) as obtained for real-time MRI with interleaved and sequential flow encoding with cine MRI recordings during free breathing. The latter approach was chosen as an established clinical reference and because cine MRI with breath holding had lower nominal in-plane and temporal resolution. For high peak velocities above 120 cm s^{-1}, both real-time MRI methods resulted in larger values than obtained for cine MRI, while lower peak velocities were similar. The correlation coefficients for real-time MRI with interleaved and sequential flow encoding vs. cine MRI were 0.90 and 0.91, respectively. Respective Bland–Altman plots of peak velocities (Fig. 4, right part) revealed a bias in peak velocity of about −7 cm s^{-1} for both real-time MRI methods. The limits of agreement for cine vs. real-time MRI were −29.2 to 15.5 cm s^{-1} for interleaved and −28.6 to 14.5 cm s^{-1} for sequential flow encoding, respectively. The internal robustness of the real-time MRI versions is well documented by very similar peak velocities. On the other hand, for cine MRI it is not clear how to identify the exact contribution responsible for the single peak velocity value as the acquisition merges data from multiple heartbeats.

Finally, Fig. 5 depicts the stroke volumes as derived from real-time MRI and cine MRI during free breathing. Slightly higher values were obtained for real-time MRI with interleaved flow encoding when compared to cine MRI. This is also seen in the Bland–Altman plot, where the differential stroke volume between cine and real-time MRI vs. the mean stroke volume yielded a bias of −5.7 mL cycle^{-1} and limits of agreement of −12.5 to 1.1 mL cycle^{-1}. On the contrary, real-time MRI with sequential flow encoding resulted in slightly lower stroke volumes than cine recordings with a bias of 3.4 mL cycle^{-1} and limits of agreement of −3.1 to 9.9 mL cycle^{-1}. Both correlation coefficients for real-time MRI with interleaved and sequential flow encoding vs. cine MRI were 0.98.

DISCUSSION

This study demonstrates the feasibility of real-time phase-contrast MRI of blood flow in the ascending aorta at high spatiotemporal resolution and adequate image quality. In comparison to conventional cine phase-contrast MRI with free breathing, real-time MRI offers a substantial gain in imaging time. Moreover, quantitative evaluations confirm the ability to obtain reliable flow parameters. Also, real-time flow MRI allows for imaging of irregular cardiovascular physiology including the responses to stress and exercise.
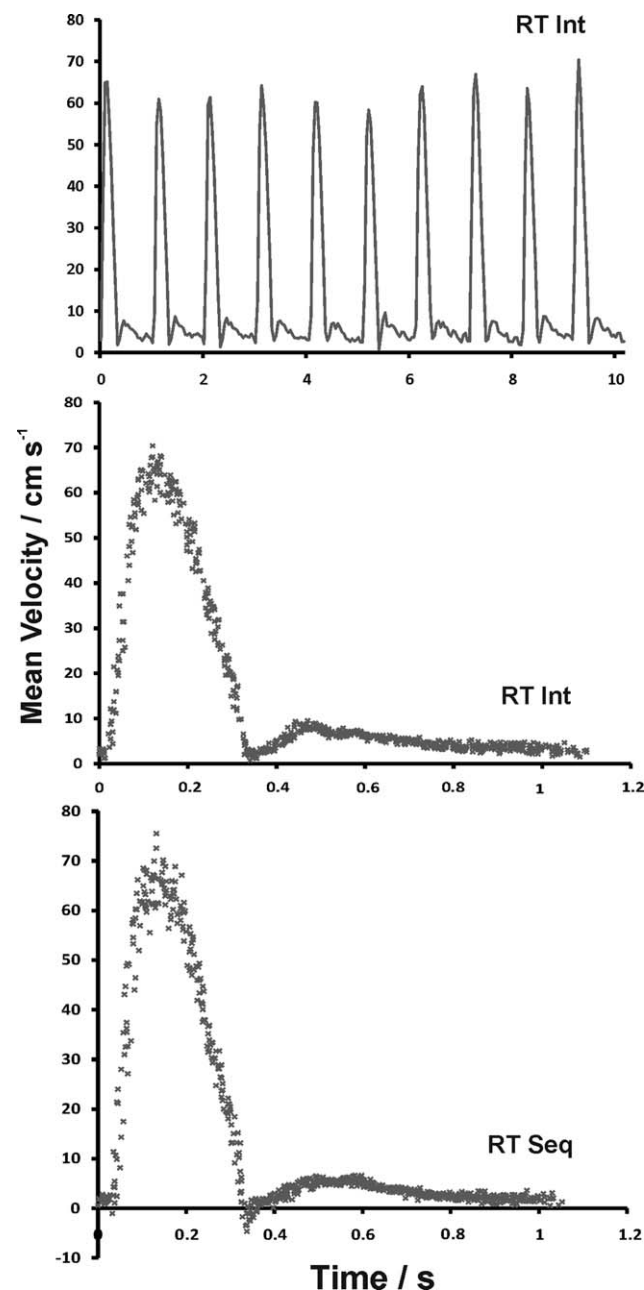
Figure 3. (Top) Mean flow velocities spatially averaged over the lumen of the ascending aorta (single subject, 10 heartbeats) as obtained by real-time MRI with interleaved flow encoding. (Middle) Mean velocities for real-time MRI with interleaved flow encoding (30 heartbeats) sorted according to the R wave and (bottom) similar data for sequential flow encoding.
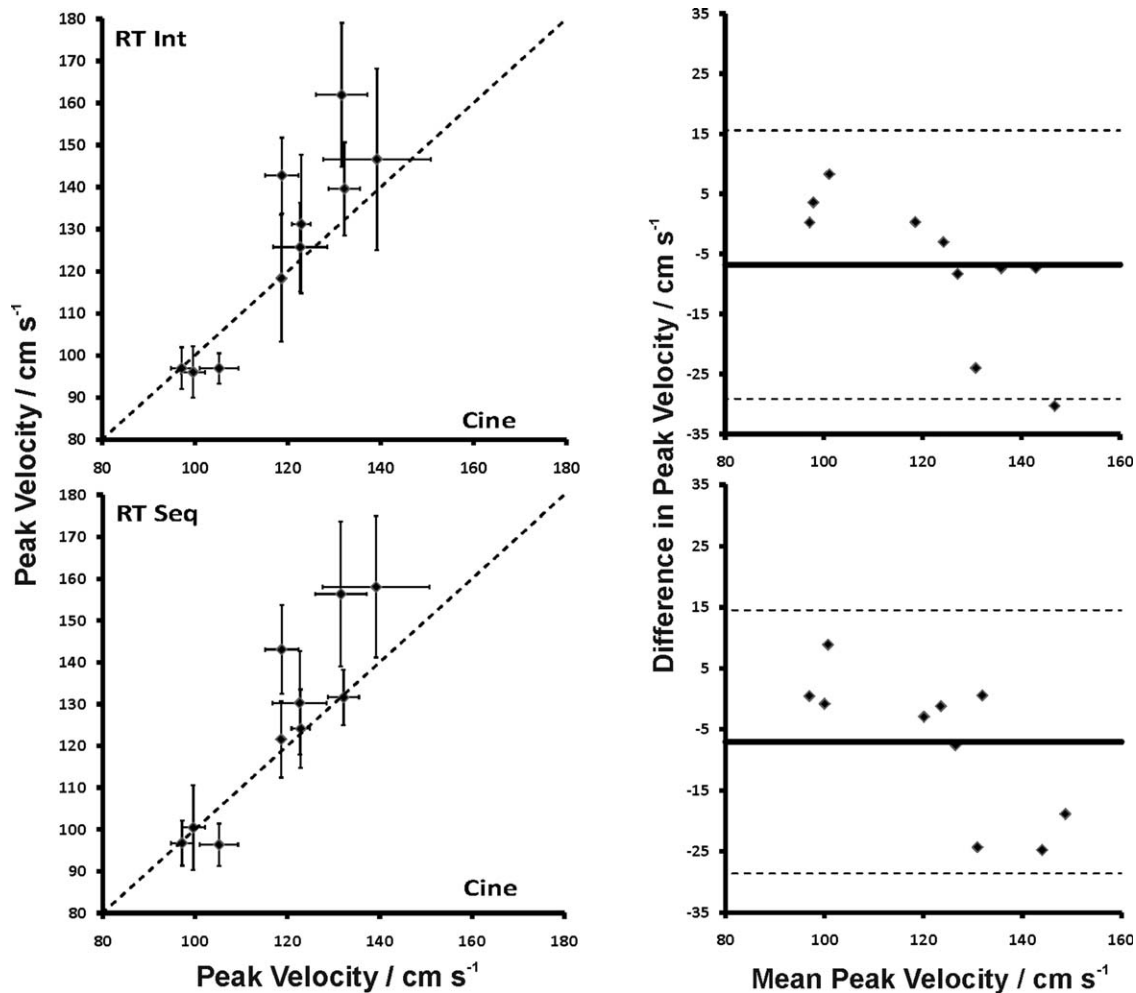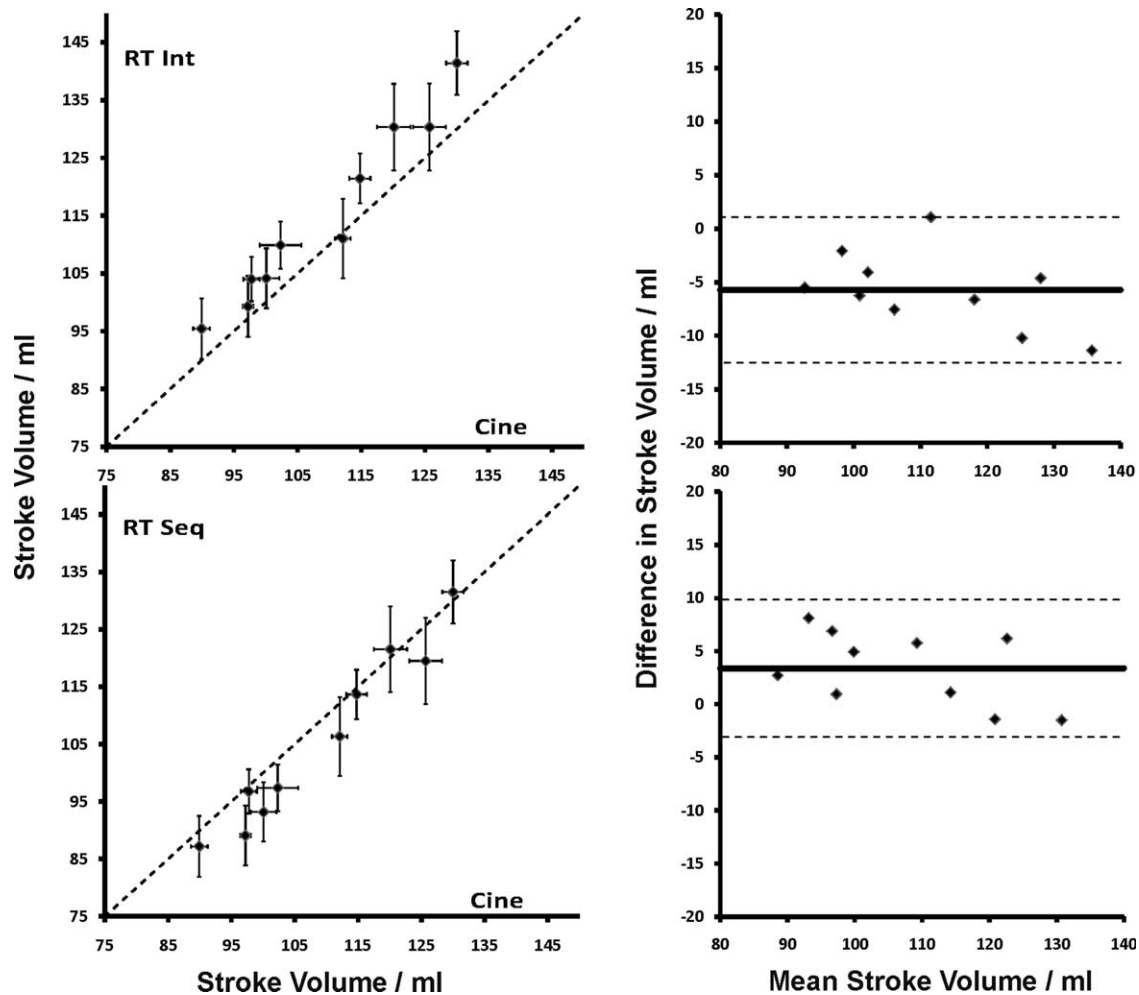
Figure 4. (Left) Peak velocities for 10 subjects (mean ± SD) as obtained for real-time MRI (averaged across 30 heartbeats) with interleaved (RT Int) and sequential (RT Seq) flow encoding vs. cine flow MRI during free breathing (averaged across three synthetic cycles). (Right) Corresponding Bland–Altman plots of the difference (cine – real-time MRI) in peak velocity. The solid lines represent mean values of -6.8 cm s^{-1} and -7.0 cm s^{-1} for interleaved and sequential flow encoding, respectively. Dashed lines refer to ±1.96 SD, indicating limits of agreement.

The real-time phase-contrast maps eventually showed residual streaking artifacts during early systole—probably due to rapid and pronounced contrast changes. However, the analysis of blood flow in the aorta was not affected. Another limitation of the proposed real-time phase-contrast MRI technique is its current lack of general availability. While the acquisition part does not require any hardware modification of existing MRI systems, sufficiently fast online reconstructions for clinical trials depend on a parallelized version of the reconstruction algorithm and its implementation on a GPU-equipped computer. Based on technical progress in our own setting we expect to achieve real-time reconstruction speed by the end of 2013. A further bottleneck is the availability of post-processing software for flow analyses that reliably deals with hundreds of images and phase-contrast maps from multiple heartbeats. The most difficult problem seems to arise from the need for a fully automated segmentation of cardiac vessels. Although the improved quality of diastolic real-time images might be helpful in this respect, foreseeable mathematical advances will have to exploit the temporal continuity

of vessel contours to ensure a reliable propagation without any manual interference.

The evaluated flow values for the ascending aorta are similar but not entirely identical for real-time and cine MRI recordings. For example, higher peak velocities for real-time MRI than for cine MRI for high-flow conditions above 120 cm s^{-1} (Fig. 4) may indeed be correct, because lower values in cine recordings cannot be excluded to be affected by phase averaging due to the use of data from multiple heartbeats. True physiological variations between heartbeats are also the most likely source for the higher standard deviations observed for real-time MRI peak velocities. These explanations are further supported by reports that cine MRI leads to lower peak velocities than observed by Doppler ultrasound techniques (4), which once again raises the question about a reliable standard of reference for in vivo flow measurements. The present results add further evidence that cine MRI methods may not be suitable for this purpose.

Another minor though apparently systematic difference was observed for real-time acquisitions with interleaved vs. sequential flow encoding, for example, when

Figure 5. (Left) Stroke volumes for 10 subjects (mean ± SD) as obtained for real-time MRI (averaged across 30 heartbeats) with interleaved (RT Int) and sequential (RT Seq) flow encoding vs. cine flow MRI during free breathing (averaged across three synthetic cycles). (Right) Corresponding Bland–Altman plots of the difference (cine – real-time MRI) in stroke volume. The solid lines represent mean values of −5.7 mL and 3.4 mL for interleaved and sequential flow encoding, respectively. Dashed lines refer to ±1.96 SD, indicating limits of agreement.

considering mean stroke volumes. These values represent the flow, which is calculated from the aortic areas and spatially averaged flow velocities, integrated over the duration of the cardiac cycle. The physical difference that may explain different mean velocities for interleaved and sequential flow encoding at any given timepoint is the actual time span over which the bipolar velocity-encoding gradient is applied to define a phase-contrast map: In our current implementation interleaved real-time MRI sequences span a period of 40 msec, while sequential versions require only 20 msec. This is because in the zero-maximum case used here the other image is without any flow-encoding gradient. Thus, the better temporal resolution for real-time MRI with sequential flow encoding resolves the brief negative undershoot after systole. This small backflow is a well-known physiological phenomenon that is caused by the rapid closure of the aortic valve and usually not seen for MRI sequences with longer velocity-encoding periods, including cine techniques.

In conclusion, real-time phase-contrast MRI of cardiovascular blood flow at 40 msec temporal resolution and 1.3 mm spatial resolution is feasible. In healthy subjects, the proposed method yields flow velocities and stroke volumes for individual heartbeats that are comparable to conventional cine MRI when averaging over multiple cardiac cycles. Further clinical validation studies are in progress.

REFERENCES

1. Nayler GL, Firmin DN, Longmore DB. Blood flow imaging by cine magnetic resonance. J Comp Assist Tomograph 1986;10:715–722.
2. Pelc NJ, Herfkens RJ, Shimakawa A, Enzmann DR. Phase contrast cine magnetic resonance imaging. Magn Reson Q 1991;7:229–254.
3. Pelc NJ, Sommer FG, Li KC, Brosnan TJ, Herfkens RJ, Enzmann DR. Quantitative magnetic resonance flow imaging. Magn Reson Q 1994;32:330–334.

4. Lotz J, Meier C, Leppert A, Galanski M. Cardiovascular flow measurement with phase-contrast MR imaging: basic facts and implementation. RadioGraphics 2002;22:651–671.

5. Gatehouse PD, Keegan J, Crowe LA, et al. Applications of phase-contrast flow and velocity mapping in cardiovascular MRI. Eur Radiol 2005;15:2172–2184.

6. Eichenberger AC, Schwitter J, McKinnon GC, Debatin JF, von Schulthess GK. Phase-contrast echo-planar MR imaging: real-time quantification of flow and velocity patterns in the thoracic vessels induced by Valsalva's maneuver. J Magn Reson Imaging 1995;5:648–655.

7. Shankaranarayanan A, Simonetti OP, Laub G, Lewin JS, Duerk JL. Segmented k-space and real-time cardiac cine MR imaging with radial trajectories. Radiology 2001;221:827–836.

8. Weiger M, Pruessman KP, Boesiger P. Cardiac real-time imaging using SENSE. Magn Reson Med 2004;51:655–660.

9. Nayak KS, Cunningham CH, Santos JM, Pauly JM. Real-time cardiac MRI at 3 Tesla. Magn Reson Med 2004;51:555–600.

10. Zhang S, Block KT, Frahm J. Magnetic resonance imaging in real time — advances using radial FLASH. J Magn Reson Imaging 2010;30:101–110.

11. Uecker M, Zhang S, Voit D, Karaus A, Merboldt KD, Frahm J. Real-time MRI at a resolution of 20 ms. NMR Biomed 2010;23:986–994.

12. Zhang S, Uecker M, Voit D, Merboldt KD, Frahm J. Real-time cardiovascular magnetic resonance at high temporal resolution: radial FLASH with nonlinear inverse reconstruction. J Cardiovasc Magn Reson 2010;12:39–46.

13. Gatehouse PD, Firmin DN, Collins S, Longmore DB. Realtime blood flow imaging by spiral scan phase velocity mapping. Magn Reson Med 1994;31:504–512.

14. Nayak KS, Pauly JM, Kerr AB, Hu BS, Nishimura DG. Real-time color flow MRI. Magn Reson Med 2000;43:251–258.

15. Klein C, Schalla S, Schnackenburg B, Bornstedt A, Fleck E, Nagel E. Magnetic resonance flow measurements in real time: comparison with a standard gradient-echo technique. J Magn Reson Imaging 2001;14:306–310.

16. Körperich H, Gieseke J, Barth P, et al. Flow volume and shunt quantification in pediatric congenital heart disease by real-time magnetic resonance velocity mapping: a validation study. Circulation 2004;109:1987–1993.

17. Nezafat R, Kellman P, Derbyshire JA, Mcveigh E. Real-time blood flow imaging using autocalibrated spiral sensitivity encoding. Magn Reson Med 2005;54:1557–1561.

18. Steeden JA, Atkinson D, Taylor AM, Muthurangu V. Assessing vascular response to exercise using a combination of real-time spiral phase contrast MR and noninvasive blood pressure measurements. J Magn Reson Imag 2010;31:997–1003.

19. Joseph AA, Merboldt KD, Voit D, et al. Real-time phase-contrast MRI of cardiovascular blood flow using undersampled radial fast low-angle shot and nonlinear inverse reconstruction. NMR Biomed 2012;25:917–924.

20. Schaetz S, Uecker M. A multi-GPU programming library for real-time applications. Lect Notes Comput Sci 2012;7439:114–128.

21. Uecker M, Hohage T, Block KT, Frahm J. Image reconstruction by regularized nonlinear inversion — joint estimation of coil sensitivities and image content. Magn Reson Med 2008;60:674–682.

22. Uecker M, Zhang S, Frahm J. Nonlinear inverse reconstruction for real-time MRI of the human heart using undersampled radial FLASH. Magn Reson Med 2010;63:1456–1462.

23. Bland MJ, Altman DG. Statistical methods for assessing agreement between two methods of clinical measurement. Lancet 1986;327:307–310.

24. Lotz J, Döker R, Noeske R, et al. In vitro validation of phase-contrast flow measurements at 3 T in comparison to 1.5 T: precision, accuracy, and signal-to-noise ratios. J Magn Reson Imaging 2005;21:604–610.

25. Gatehouse PD, Rolf MP, Graves MJ, et al. Flow measurement by cardiovascular magnetic resonance: a multi-centre multi-vendor study of background phase offset errors that can compromise the accuracy of derived regurgitant or shunt flow measurements. J Cardiovasc Magn Reson 2010;12:5–8.